

ORIGINAL RESEARCH REPORT

Scale-up manufacturing of gelatin-based microcarriers for cell therapy

Pere Dosta^{1,2} | Shiran Ferber^{1,2} | Yi Zhang^{1,2} | Kui Wang^{1,2} | Albert Ros^{1,2} |
 Nicholas Uth³ | Yonatan Levinson³ | Eytan Abraham³ | Natalie Artzi^{1,2,4}

¹Institute for Medical Engineering and Science, Massachusetts Institute of Technology, Cambridge, Massachusetts

²Department of Medicine, Division of Engineering in Medicine, Brigham and Women's Hospital, Harvard Medical School, Boston, Massachusetts

³Research and Technology, Walkersville, Maryland

⁴Broad Institute of Harvard and MIT, Cambridge, Massachusetts

Correspondence

Natalie Artzi, Department of Medicine, Division of Engineering in Medicine, Brigham and Women's Hospital, Harvard Medical School, Boston, Massachusetts, USA
 Email: nartzi@mit.edu, nartzi@bwh.harvard.edu

Funding information

Lonza

Abstract

Microcarriers, including crosslinked porous gelatin beads (Cultispher G) are widely used as cell carriers for cell therapy applications. Microcarriers can support a range of adherent cell types in stirred tank bioreactor culture, which is scalable up to several thousands of liters. Cultispher G in particular is advantageous for cell therapy applications because it can be dissolved enzymatically, and thus cells can be harvested without the need to perform a large-scale cell-bead filtration step. This enzymatic dissolution, however, is challenged by the slow degradation of the carriers in the presence of enzymes as new extracellular matrix is being deposited by the proliferating cells. This extended dissolution time limits the yield of cell recovery while compromising cellular viability. We report herein the development of crosslinked porous gelatin beads that afford rapid, stimuli-triggered dissolution for facile cell removal using human mesenchymal stem cells (hMSC) as a model system. We successfully fabricated redox-sensitive beads (RS beads) and studied their cell growth, dissolution time and cell yield, compared to regular gelatin-based beads (Reg beads). We have shown that RS beads allow for much faster dissolution compared to Reg beads, supporting better hMSC detachment and recovery following 8 days of culture in spinner flasks, or in 3L bioreactors. These newly synthesized RS beads show promise as cellular microcarriers and can be used for scale-up manufacturing of different cell types while providing on-demand degradation for facile cell retrieval.

KEYWORDS

bioreactor, hMSC, microcarriers, redox sensitive, scale-up

1 | INTRODUCTION

Cell therapy is a subtype of regenerative medicine, where stem cells are introduced into a patient to treat a disease, repair or regenerate tissue, with or without gene therapy. Human mesenchymal stem cells (hMSCs) are considered a promising candidate in cell therapy owing to their ability to self-renew and differentiate into various specialized cell types under certain physiological conditions and cues (Wei et al., 2013). hMSC can be easily isolated from different tissues (Romanov, 2003; Zuk et al., 2002) (such as bone marrow, adipose

tissue, the umbilical cord, fetal liver, muscle, and lung) and can be successfully expanded *in vitro* to be used for regenerative medicine (Bianco, Robey, & Simmons, 2008; Pittenger, 1999), as can be seen by the increase in the number of clinical trials using hMSC since 2004 (Squillaro, Peluso, & Galderisi, 2016; Wei et al., 2013) (<http://clinicaltrials.org>). For instance, hMSCs have been shown to be effective in the treatment of tissue injury, myocardial ischemia, and degenerative diseases (Abdallah & Kassem, 2009; Lee et al., 2009). Due to their low immunogenicity, hMSCs have been developed into allogeneic, off-the-shelf therapies. Indeed, one example is Mesoblast's TEMCELL

MSC product, which has received full regulatory approval in Japan to treat graft versus host disease (Sheridan, 2018). In addition, hMSC secrete a wide range of biological molecules, able to exert therapeutic effects. The most well studied are secretory trophic factors, exosomes, hormones, and cytokines (Abbasi-Malati, Roushandeh, Kuwahara, & Roudkenar, 2018; Bai et al., 2017; Prockop, 2007). For example, it has been demonstrated that exosome secreted by hMSC reduces myocardial infarction (Lai et al., 2010). Therefore, hMSC can be considered as living, dynamic, and responsive drugs that can produce a variety of therapeutic agents in response to disease-specific cues.

Large-scale and cost-effective hMSC cell expansion are needed for clinical implementation. One major challenge is their manufacturing, where product quality and reproducibility is one of the main bottlenecks (Salmikangas et al., 2015; Stephenson & Grayson, 2018). Bioreactors have been employed to provide cost-efficient processing, high yield, and large-scale capacity. In addition, bioreactors present controlled bioprocesses that are able to guarantee the production of cell-based therapies with robust *in vivo* performance (Hourd, Ginty, Chandra, & Williams, 2014; Kaiser et al., 2015; Salmikangas et al., 2015). However, since hMSC are adhesion dependent and cannot be grown in suspension, their scale-up is more challenging. During the last decade, a large range of bioreactor culture systems, such as microcarrier-based stirred tank reactors (dos Santos et al., 2014), hollow fiber (Nold, Brendel, Neubauer, Bein, & Hackstein, 2013), rotating wall vessels (Varley, Markaki, & Brooks, 2017), and perfusion bioreactor (Nguyen, Ko, & Fisher, 2016) have been designed to support hMSC expansion. These bioreactors were combined with different scaffold structures to support cell growth, where microcarriers seem to be one of the most promising vehicles as they can support cell growth in large bioreactor volumes (Lambrechts et al., 2016). Due to their high surfacetovolume ratio, microcarriers offer large surface area for cell expansion in a small and efficient footprint (Hervy et al., 2014; Wu, Liu, & Lian, 2004). For hMSC production, collagen-coated Cytodex-3 (Chen, Chew, Tan, Reuveny, & Steve Kah Weng, 2015) and gelatin-coated Cultispher (Sun et al., 2010) microcarriers are most typically used. Cytodex-3 is a cross-linked dextran matrix with a gelatin coating, while Cultispher is a porcine gelatin-based porous microsphere. The porous nature of Cultispher microcarriers affords high cell:bead loading compared with Cytodex microcarriers (Ng, Berry, & Butler, 1996). Cultispher microcarriers present three distinct advantages: (a) porous structure that significantly increases the area available for cell attachment and proliferation; (b) gelatin-based (derived from collagen)—one of the main components of the extracellular matrix (ECM)—providing with binding motifs (RGD sequence) for cells to attach to. Therefore, multiple integrins can bind to the RGD motif, facilitating cell adhesion (Barczyk, Carracedo, & Gullberg, 2010; Davidenko et al., 2016; Muñoz, Shih, & Lin, 2014). (c) Enable facile cell removal—the crosslinked gelatin can be dissolved by the addition of proteolytic enzymes while maintaining cell viability. However, due to the production of ECM by the highly dense cells that further proliferate over time, complete dissolution of the microcarriers and liberation of

the cells requires a long time, negatively affecting cell viability and yield. Alternatively, it was reported that nonenzymatic cell harvesting procedure can be used (Nienow, Rafiq, Coopman, & Hewitt, 2014). For instance, microcarriers coated with a thermo-responsive polymer can release the cells in response to temperature change; however, this approach requires polymeric coating of the microcarrier, which may affect its cell-adhesive properties, limiting its applicability (Yang, Jeon, Bhang, Lee, & Kim, 2010). Addressing these concerns for the Cultispher beads, we propose the design of stimuli-triggered fast dissolving beads. We successfully fabricated redox-sensitive beads (RS beads) without altering the physical properties of the regular Cultispher beads (Reg beads). RS beads were able to considerably reduce the dissolution time (from 56 to 8 min with cell concentration of 1 million/ml) using a noncytotoxic dissolution solution. Therefore, these on-demand degrading microcarriers can be used to scale-up hMSC manufacturing in large bioreactors, increasing their potential use in clinical applications.

2 | METHODS

2.1 | Materials

Reagents and solvents used for polymer synthesis were purchased from Sigma-Aldrich. Reg beads (Cultispher G), and noncrosslinked gelatin beads were obtained from Lonza. Spinner flasks were obtained from Corning (Corning 125 ml Disposable Spinner Flask with 70 mm Top Cap and 2 Angled Sidearms). For *in vitro* studies, hMSC cell line was obtained from ATCC (Manassas, VA) and maintained at 37°C in 5% CO₂ atmosphere in complete DMEM, containing 10% fetal bovine serum, 100 units ml⁻¹ penicillin, 100 µg ml⁻¹ streptomycin, 0.1 mM MEM nonessential amino acids, and 2 mM L-glutamine obtained from Gibco.

2.2 | Synthesis of redox-sensitive crosslinker

Redox-sensitive crosslinker was fabricated by diphosgene chemistry. Briefly, 2.25 g (10 mmol) of cystamine 2-HCl was deprotonated with 40 ml of 1 M NaOH and 20 ml of DCM in 100 ml glass beaker and the organic phase containing the product of interest was collected and dried using Na₂SO₄. For cystamine isocyanation, 8.75 g (40 mmol) of 1,8-bis(dimethylamino)-naphthalene (BDN) was mixed with cystamine and added dropwise for 2 min under agitation at 800 rpm to 985 µl (8.16 mmol) of diphosgene mixed with 30 ml of DCM (diphosgene was previously immersed into ice for 30 min). The solution was allowed to react for two more minutes after full addition of cystamine in ice and two extra minutes at room temperature. After that, the reaction was quenched by the addition of 50 ml of 1 M HCl and 20 ml of DCM, and the organic phase containing the product of interest was collected. Finally, 1,2-bis(2-isocyanatoethyl) disulfide product (organic phase) was purified with three washes of 50 ml HCl 1 M following of one wash of 50 ml NaOH 1 M. 1,2-Bis(2-

isocyanatoethyl) disulfide product was dried using Na_2SO_4 , and organic solvent was removed. The 1,2-bis(2-isocyanatoethyl) disulfide product was characterized by nuclear magnetic resonance ($^1\text{H-NMR}$) spectroscopy using chloroform-*d* as a solvent and Fourier transform infrared spectroscopy (FTIR) spectrophotometer.

2.3 | Redox-sensitive microcarrier synthesis

RS beads were synthesized by crosslinking gelatin beads with 1,2-bis(2-isocyanatoethyl) disulfide. A total of 10 g of noncrosslinked beads were mixed during 60 min at 370 rpm with 120 ml of acetone and 30 ml of 0.12 M sodium acetate trihydrate at pH 8.5. Once gelatin beads were hydrated, 0.41 g (2 mmol) of 1,2-bis(2-isocyanatoethyl) disulfide and 50 μl (0.4 mmol) of triethylamine were added, allowing to react for 105 min at 450 rpm. After that, beads were allowed to sediment for 15 min and supernatant was removed to eliminate the nonreacted crosslinker. The microcarriers were washed three times with 600 ml of acetone for 15 min at 450 rpm. Finally, nonwashed crosslinker was deactivated using 100 ml of deionized (DI) water at pH 8.5 containing 1.52 g (20 mmol) of glycine for 60 min under agitation. RS beads were allowed to sediment overnight at 4°C for further purification.

2.4 | Purification of the redox-sensitive microcarriers

RS beads were purified following three different procedures. First, the microcarriers were washed three times with 400 ml of water during 60 min at 500 rpm. The first wash was performed using water at 25°C, the second wash at 55°C, and third wash at 25°C. After water purification, microcarriers were purified three times with 200 ml of methanol. In the first and second washes, methanol was added and the mixture was stirred at 500 rpm for 60 min. The third wash was performed at 70°C and the mixture was stirred at 500 rpm for 60 min. Then, the microcarriers were allowed to sediment, cool down to room temperature, and the supernatant was removed. Finally, the microcarriers were washed twice with 200 ml of acetone for 60 min at 500 rpm and twice with 100 ml for 15 min. After the last wash, the resultant microcarriers were placed into a vacuum oven overnight to dry the remaining solvent.

2.5 | Redox-sensitive microcarriers labeling

Noncrosslinked beads, Reg beads, and RS beads were fluorescently labeled with Fluorescein isothiocyanate dye (FITC). Microcarriers were dissolved at 20 mg/ml in phosphate buffer saline (PBS) at pH 7.4 and 5 mg of FITC dissolved in PBS at pH 7.4 was added dropwise to the microcarriers, allowing to react overnight at 4°C. To remove the free dye the microcarriers were washed twice with PBS at pH 7.4.

2.6 | Microscope and scanning electron microscopy microcarriers characterization

FITC labeled-microcarriers were mixed with Tissue Tek in a plastic mold and were kept at -80°C overnight for microscopy studies. Cryosections of 10 μm in thickness were performed. Each microcarrier sample was analyzed by microscopy at $\times 4$ and $\times 10$ magnification.

For scanning electron microscopy (SEM), samples were diluted in DI water (100 mg/ml) and 100 μl suspension was smeared onto an SEM stub and allowed to air dry overnight. SEM image of the beads was taken under high vacuum mode.

2.7 | Extraction and swelling studies of the microcarriers

100 mg/ml of Reg beads and RS beads were hydrated overnight with PBS at 4°C. A total volume of 1 ml of beads (100 mg) were added into pre-weighted Eppendorf tube (W_o) and was placed into 55°C water bath. After, 6, 12, and 24 hr, beads were allowed to settle, and supernatant was carefully removed. Each Eppendorf tube containing wet beads was weighted (W_w). Then, the beads were washed with DI water twice, the supernatant was carefully removed, and the final sample was lyophilized. Finally, the weight of each tube with dry beads was measured (W_d). To determine the extraction percentage, the following calculation was carried out: $(W_d - W_o)/100 \text{ mg} \times 100\%$. To determine the swelling ratio, the following calculation was carried out: $(W_w - W_o)/100 \text{ mg} \times 100\%$.

2.8 | Viability assay of reducing agents and dissolution enzymes in hMSC

Cell viability assays of treated cells was performed using the MTS assay (CellTiter 96 AQueous One Solution Cell Proliferation Assay, Promega Corporation) as instructed by the manufacturer. Briefly, cells were seeded in 96-well plates at 10,000 cells/well and incubated overnight to roughly 80% confluence prior to performing the experiments. Reducing agents and dissolution enzymes were added to the cells at different concentrations and for different periods of time. Then, the medium was removed, cells were washed with PBS, and complete medium supplemented with 20% MTS reagent (vol/vol) was added. Cells were incubated at 37°C, and absorbance was measured at 490 nm using a microplate reader.

2.9 | Microcarriers dissolution using enzymes and/or reducing agents

To assess the beads dissolution mechanism, microcarriers were hydrated with DPBS (with Ca^{2+} and Mg^{2+}) at a concentration of 20 mg/ml for 12 hr at 4°C. A total volume of 0.5 ml of beads (10 mg) were treated with different enzymes or/and reducing agent, such as

tris(2-carboxyethyl)phosphine hydrochloride (TCEP) at 37°C. Microcarriers dissolution time was determined by visual inspection and under the microscope.

2.10 | Culturing hMSC on porous gelatin beads in 125 ml spinner flasks

Previous to hMSC culture in spinner flasks, microcarriers were pretreated. A total volume 2 g/L microcarriers were hydrated at 4°C with PBS 1X for 12 hr. After that, microcarriers were washed twice with 30 ml of complete hMSC media and resuspended at final concentration of 25 mg/ml. Then, 8 ml of microcarriers were added to the spinner flask containing 92 ml of complete hMSC medium, to ensure a final concentration of 2 mg/ml. Once the spinner flask was placed on the magnetic stirrer platform in a humidified incubator at 37°C, 20,000 hMSC cells/ml were inoculated. To culture hMSC in spinner flasks, agitation was turned on for 10 min at 35 rpm and off for 90 min within the first 5 hr, allowing adequate cell–microcarrier interactions. After that, the spinning speed was increased by 15 rpm every 24 hr after Day 3, as summarized in the Supplementary Table S1. Media exchange is performed as a percentage of the working volume. No media exchange was performed during the first 3 days; then, 85% of the media was exchanged (once per day) from Day 4 to Day 7 and 75% of the media was exchanged (twice per day) from Day 8 to Day 9, as shown in the Supplementary Table S2.

2.11 | hMSCs counting protocol from spinner flasks

To assess the hMSC counts, 1 ml of sample was analyzed for each spinner flask. Samples were dissolved with reducing agents and/or dissolution enzymes following the procedure that previously has been described. Once all beads were dissolved (by visual inspection), cell count was performed.

2.12 | Culture of hMSCs in 3 L bioreactors

Bioreactor tests were performed in 3 L Eppendorf BioBLU vessels. For each run, two vessels were set up—a control vessel with Reg beads and a test vessel with RS beads. Prior to culture, microcarriers were hydrated at 4°C using DPBS (+/+) (Gibco) for 12–24 hr, then transferred into a 1 L volume of 2 g/L glucose serum-containing media (Lonza MSCBM-CD, 1% Lonza MSCGM-CD, 2% Hyclone FBS, 25 µg/L Lonza Gentamicin Sulfate). Aside from the microcarriers used, the vessels were set up and operated under the same conditions. Bioreactor control was achieved using HyPerforma G3 Lab Controllers and TruBio Software (ThermoFisher). Set points for control were set for temperature (37°C), pH (7.2), and %DO (50%). Air was pumped continuously into the system at a rate of 0.1 L/min. Nitrogen and oxygen gasses were pumped in to control %DO of the system. CO₂ was pumped in as

necessary to maintain media pH. Intermittent agitation was used for the first 6.8 hr of culture (0 RPM for 60 min, then 50 RPM for 10 min, alternating). Afterward, agitation was ramped from 55 to 100 rpm over time. Cells were cultured in 3D for up to 8 days in serum-containing media with 4 g/L microcarriers. Starting on Day 4, continuous media exchange with a 4 g/L glucose equivalent media was initiated at a rate of one vessel volume per day.

2.13 | Sampling from 3 L bioreactor

A total volume of 5 ml samples were taken daily from each vessel for pH and nutrients/metabolites measurements using a NOVA BioProfile FLEX (NOVA biomedical). In addition, samples were drawn on Days 1, 4, and 6 to monitor cell growth over time. Samples were washed in DPBS (–/–) and incubated with dissolution reagent in a 1:1 volume at 37°C until microcarriers were dissolved. To facilitate dissolution, the samples were pipetted repeatedly using a 10 ml serological pipette in 10-minute increments. Once dissolved, the samples were vortexed then drawn into a Via1-Cassette (Chemometec) containing Acridine Orange and DAPI stains. Each cassette was read using a Nucleocounter NC-200 (Chemometec) to determine cell density and viability.

2.14 | Harvesting the 3 L bioreactor

On Day 7 of culture, a 1 L sample was taken from the vessel for harvesting. The harvest material was drained of media and washed once with 600 ml of DPBS (–/–). The volume was reduced to 300 ml, the dissolution reagent was added, and the system was incubated for 5 min. The RS bead dissolution reagent used was 10 mM TCEP with Trypsin (0.025%). To expedite dissolution of the microcarriers when harvesting the bioreactors, mechanical force was utilized in addition to chemical means. While incubating with the dissolution reagents, the dissolving microcarriers were continuously pumped through a closed-loop assembly of specialized tubing designed to break up microcarrier aggregates through shear. In order to estimate the number of passes through this assembly, we defined a simple measurement of “volumes processed”: the unit of time needed to pass the entire bioreactor through the assembly once (e.g., 1 L circulating at 100 ml/min for 30 min = 3 “volumes processed”). Assuming that passing through this assembly is the rate-limiting step of microcarrier dissolution, the process would be scaled up by keeping volumes processed, rather than time, constant.

The system was incubated for 5 min before initiating the pump for the tubing assembly loop. Samples were taken from bioreactor over the course of dissolution to monitor progress and determine when it was complete. Degree of dissolution of the sample was determined by measuring cell density and viability using the NC-200 and visual inspection using a light microscope. A vessel was considered fully dissolved once the cells released into suspension plateaued and there were no aggregates observed under microscope. Once fully dissolved, the vessel was drained, and a final sample was drawn.

3 | RESULTS

We developed redox-sensitive crosslinked porous gelatin beads for the scale-up manufacturing of cells that afford stimuli-triggered microcarrier dissolution for facile cell retrieval. As a proof of concept, our newly developed RS beads have been synthesized (Figure 1a,b) and tested for hMSC expansion in bioreactors (Figure 1c). We hypothesized that the surface modification of the microcarriers (RS beads) would not alter cell attachment as compared with Cultispher-G beads (Reg beads), thus promoting cell proliferation. We found that cells could attach to the RS beads, proliferate and then be rapidly retrieved using a well-defined dissolution medium to degrade the beads, achieving high yield of cell recovery.

3.1 | Development of fast-dissolving, RS beads

Synthesis of RS beads was performed via a two-step procedure. First, cystamine isocyanate crosslinker was obtained reacting cystamine with diphosgene in presence of 1,8-bis (dimethylamino)-naphthalene (Figure 2a), allowing their reaction with the noncrosslinked gelatin (Sigurdsson, Seeger, Kutzke, & Eckstein, 1996). The resulting crosslinker was characterized in terms of its molecular structure by $^1\text{H-NMR}$ and FTIR. The $^1\text{H-NMR}$ spectra showed that peaks for $-\text{CH}_2\text{CH}_2-$ have shifted to low magnetic field, indicating the conversion from $-\text{NH}_2$ to $-\text{NCO}$. The FTIR spectra confirmed the successful synthesis by showing specific peak of isocyanate at $2,270\text{ cm}^{-1}$, and the absence of specific peaks for amine at $1,610$ and $3,340\text{ cm}^{-1}$

(Supplementary Figure S1). After successful synthesis of a redox-sensitive crosslinker, RS beads have been fabricated following the procedure previously described in materials and methods (Figure 2b).

3.2 | Biophysical characterization of RS beads

The size of the new redox-sensitive microcarriers was comparable to that of the Reg beads, as seen by SEM (Figure 3a), and by fluorescence imaging (Figure 3b). The latter was performed after the samples were suspended in FITC solution (0.1 mg/ml) and incubated under 4°C overnight. To further study the physical properties of Reg beads and RS beads, extraction and swelling studies in DPBS have been performed. Both microcarriers similarly showed a decrease of 10% in total mass following extraction and a 10% increase in weight owing to swelling (Figure 3c).

3.3 | RS beads afford faster dissolution than Reg beads

Reg beads and RS beads dissolution times were tested using a combination of enzyme and reducing agent, or enzyme alone (Figure 4a). Full dissolution was reached for Reg beads after 30 min in enzyme solution (0.5 U/ml Clzyme BP Protease and 0.5 U/ml Clzyme collagenase), and they could not be dissolved in the presence of reducing agents only, as expected. In contrast, the dissolution time of RS beads was 20 min in the presence of enzyme alone and about 70 min in the presence of

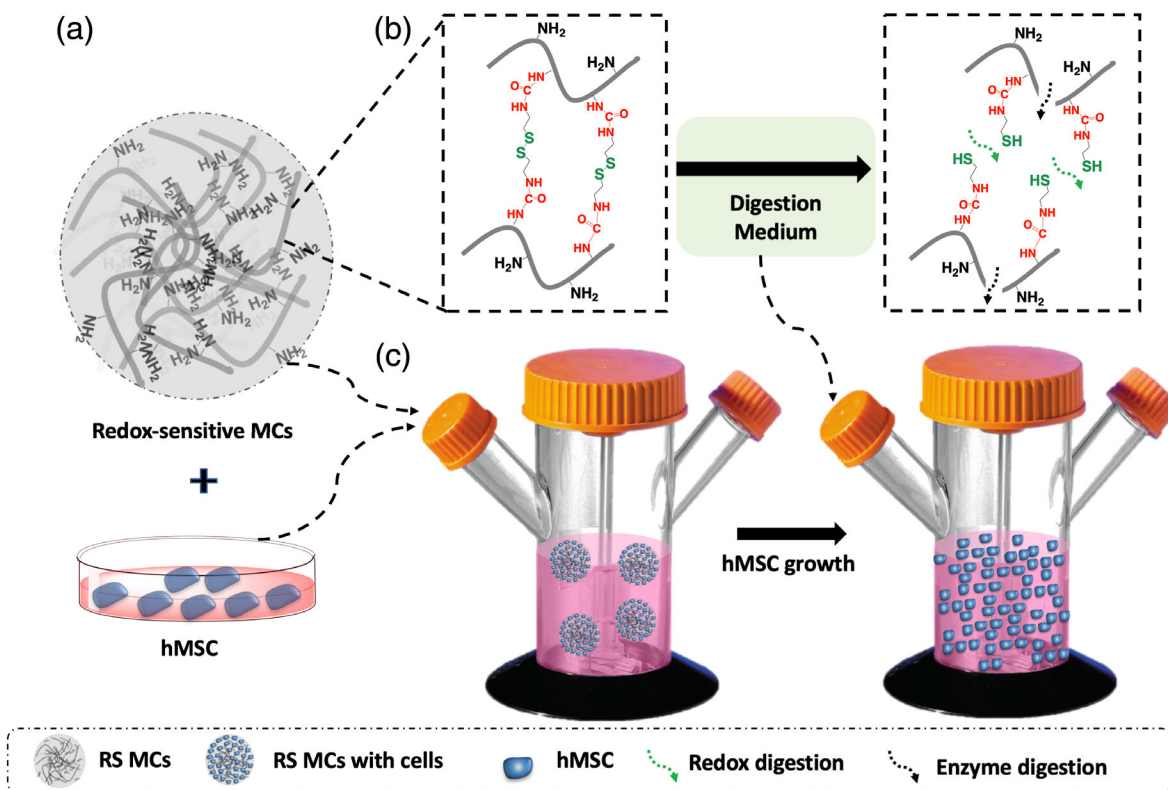


FIGURE 1 (a) Schematic illustration of RS beads, (b) their dissolution mechanism, and (c) their scale up in bioreactors

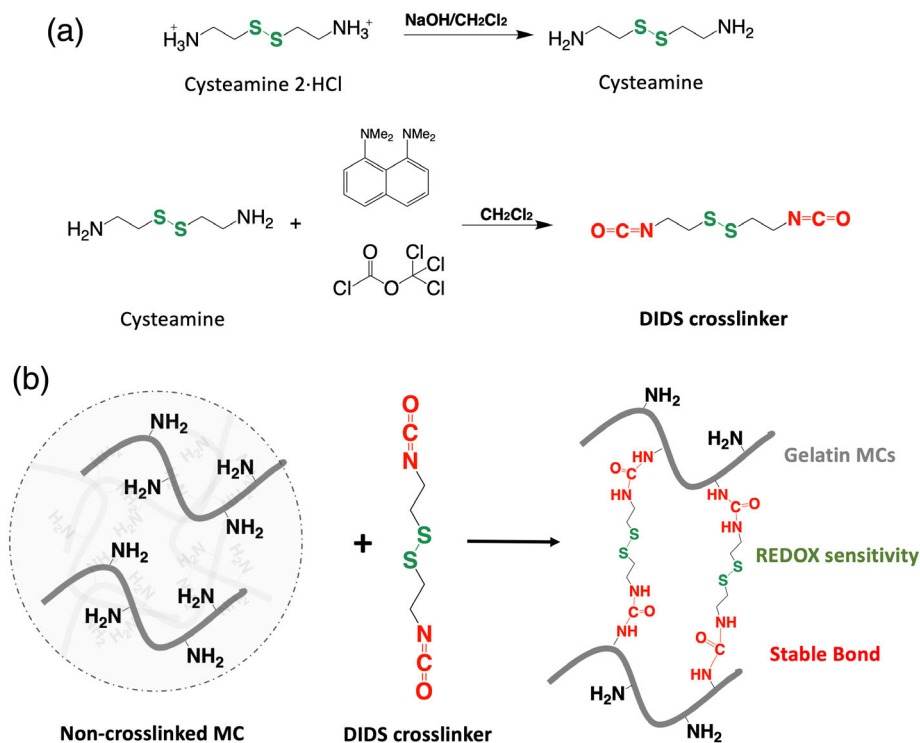


FIGURE 2 (a) Synthesis of a redox-sensitive crosslinker 1,2-bis(2-isocyanatoethyl) disulfide (DIDS). (b) Synthesis of redox-sensitive beads (RS beads)

reducing agent alone. The mixture of reducing agents and enzyme, however, enabled bead dissolution within 6 min, confirming that RS beads dissolution is carried out by two different mechanisms—redox and enzymatic degradation. In contrast, the Reg beads did not reach full dissolution in the same time frame when a mixture of reducing agent and enzyme was used (Figure 4b).

Once microcarrier dissolution conditions were optimized, the cytotoxicity of the dissolution solution and the RS beads dissolution products has been studied by MTS assay using hMSC. Figure 4c shows that with treatment time lower than 60 min, hMSC tolerated all the dissolution solutions. No toxicity was observed when enzyme alone, reducing agent alone, or the combination of enzyme with reducing agent were used. In addition, different concentrations of reducing agent were tested (Supplementary Figure S2), showing that there was no toxicity, even with high concentration of reducing agent (50 mM), when treatment duration was less than 30 min. For longer treatment time, hMSC had low viability (between 80 and 85%), at a high concentration of reducing agent (50 mM). These results suggest that higher concentration of reducing agent solution could be employed as a dissolution solution postulating that dissolution time can be significantly reduced.

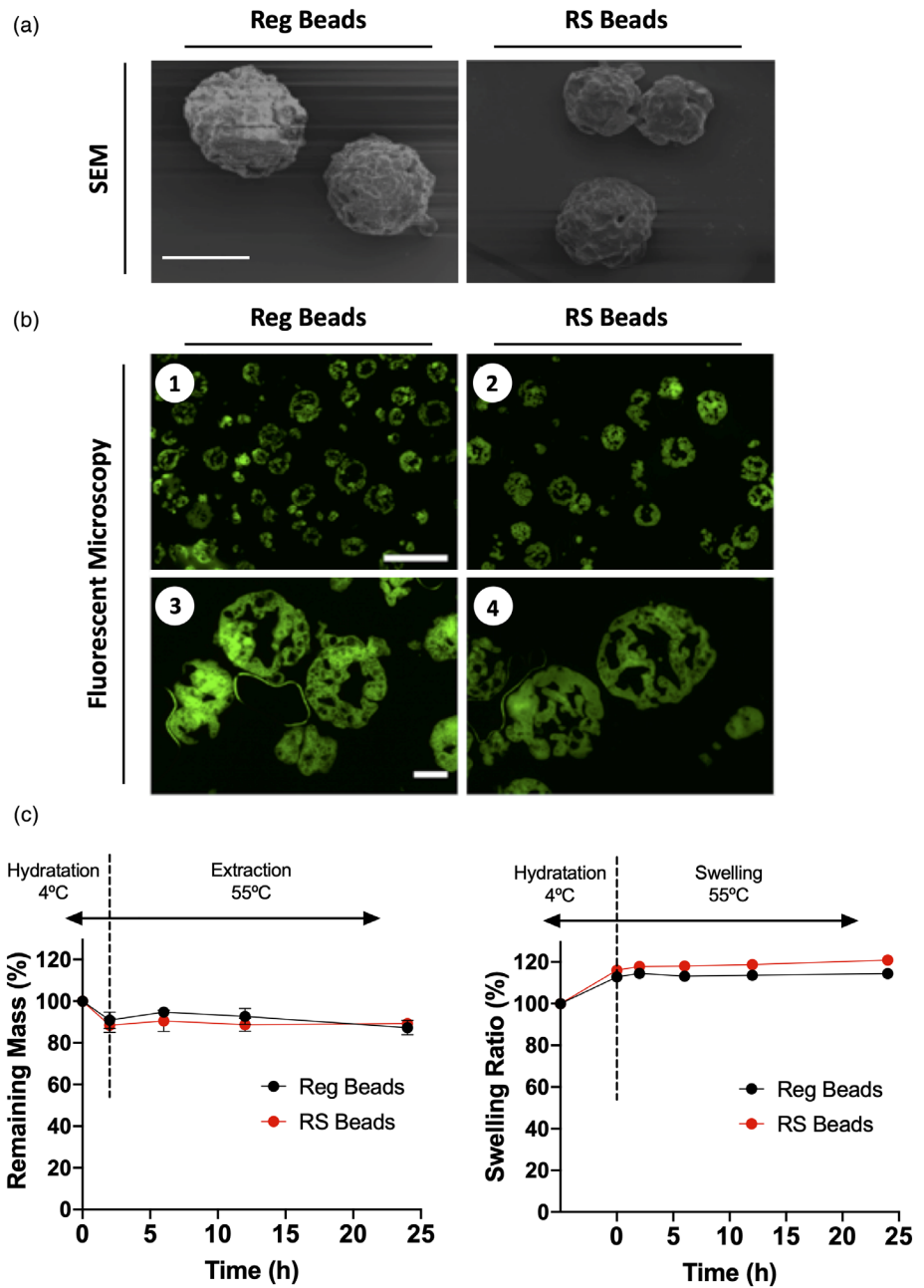
3.4 | Spinning culture of hMSC and dissolution studies

hMSC were cultured and expanded using our newly developed RS beads in spinning flasks. Cell culture conditions, such as cell density and spinning speed, have been optimized to achieve high rate of hMSC expansion. A step function was found to be optimal with regard to the spinning speed; hence, the spinner was turned on for 10 min at

35 rpm and then off for 90 min within the first 5 hr, allowing for adequate cell–microcarrier interactions and avoiding microcarrier aggregation. Then, the spinner speed was fixed at 50 rpm until Day 3. Lastly, the spinning speed was increased by 15 rpm every 24 hr after Day 3 for the remaining culture period (Figure 5a). The increased shear force helps limit beads aggregation. Once the cell culture conditions were optimized, cell density was determined every day, validating that hMSC had comparable growth rate when attached to Reg beads and RS beads. After the beginning of media exchange on Day 4, cell number increased exponentially for both microcarriers (Figure 5b). In addition, microcarrier dissolution time was determined at different time points during the hMSC culture. A mixture of reducing agent with enzyme was used to dissolve RS beads and only enzyme was used to dissolve the Reg beads. Results show that dissolution time increased in proportion to cell concentration for Reg beads (from 26 to 55 min). In contrast, when RS beads were used, lower dissolution times were observed for all time points (from 12 to 22 min) (Figure 5c). To further confirm the microcarriers cell adhesion, the microcarriers were stained with DAPI at different time points (3, 5, 7, and 9 day). Results showed that cell number is increased over time, showing high density of cells at Days 7 and 9 (Figure 5d).

Although RS beads exhibit much faster dissolution time in solution compared to the enzymatic dissolution of the Reg beads, there are still several factors that can be used to further reduce the dissolution time of the RS beads. For example, the concentration of the reducing agent can be increased, and its high stability enables its synergistic use along with other cell dissolution/detachment agents, such as trypsin and sodium citrate buffer. In the following studies, various dissolution solutions have been applied to RS beads. These studies indicate that both trypsin (0.025%) and sodium citrate (0.015 M) with

FIGURE 3 Biophysical characterization of RS beads. (a) scanning electron microscopy (SEM) images of both Reg beads and RS beads. Scale bar 200 μm . (b) Fluorescent images of Reg beads (1); RS beads (2). Scale bar 500 μm . The corresponding beads under high magnification (3,4). Scale bar 100 μm . (c) Extraction (left) and swelling (right) studies for Reg beads and RS beads in DPBS. Results are shown as mean and standard deviation (SD) of quadruplicates



10 mM of reducing agent were able to improve the dissolution of RS beads. The dissolution time decreased from 22 to 16 min using sodium citrate, and 12 min with trypsin. In addition, when 20 mM of reducing agent was used the dissolution time was further reduced to 15 min with sodium citrate, and 8 min with trypsin. Cell viability was quantified after full dissolution to study whether cytotoxicity is imparted by the cell detachment agents. Figure 6a,b shows that 0.015 M sodium citrate solutions present some level of cytotoxicity to hMSC, making them not a good candidate for microcarriers dissolution. In contrast, no cell toxicity was observed using trypsin. It is noteworthy that with 12 min exposure to 0.025% trypsin and 10 mM reducing agent, hMSC still has high viability, over 90%, confirming that this dissolution solution can be further used to achieve a fast and safe dissolution of RS beads.

3.5 | hMSC production in large bioreactors

Once the *in vitro* experiments in spinner flasks have been optimized, the RS beads were used for hMSC production in large bioreactors. Cell growth, cell attachment, cell viability, and dissolution time were studied and compared between Reg beads and RS beads.

Cell growth curves showed no significant hMSC proliferation differences between Reg beads and RS beads during the entire study. Similar to spinner flask experiments, exponential cell growth was observed after Days 4–5 of culture. By Day 7 of culture, hMSC concentration reach $0.65\text{E} + 06 \pm 0.16\text{E} + 06$ cell/ml and $0.55\text{E} + 06 \pm 0.14\text{E} + 06$ cell/ml using Reg beads and RS beads, respectively (Figure 7a). In addition, hMSC attachment to the microcarriers was confirmed by microscopy on Days 1 and 4 (Figure 7b), showing non-significant differences. Microcarriers were harvested at Day

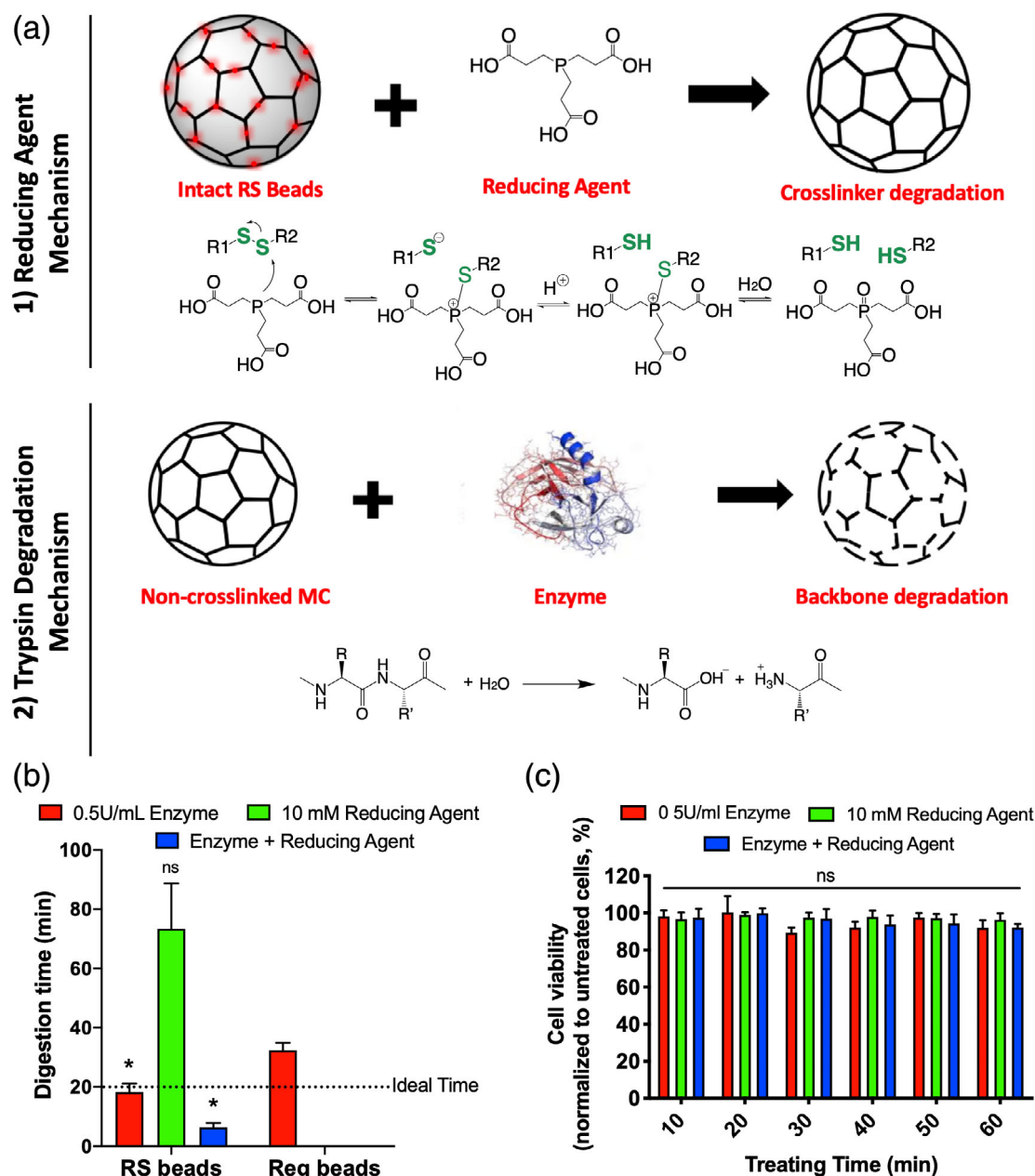
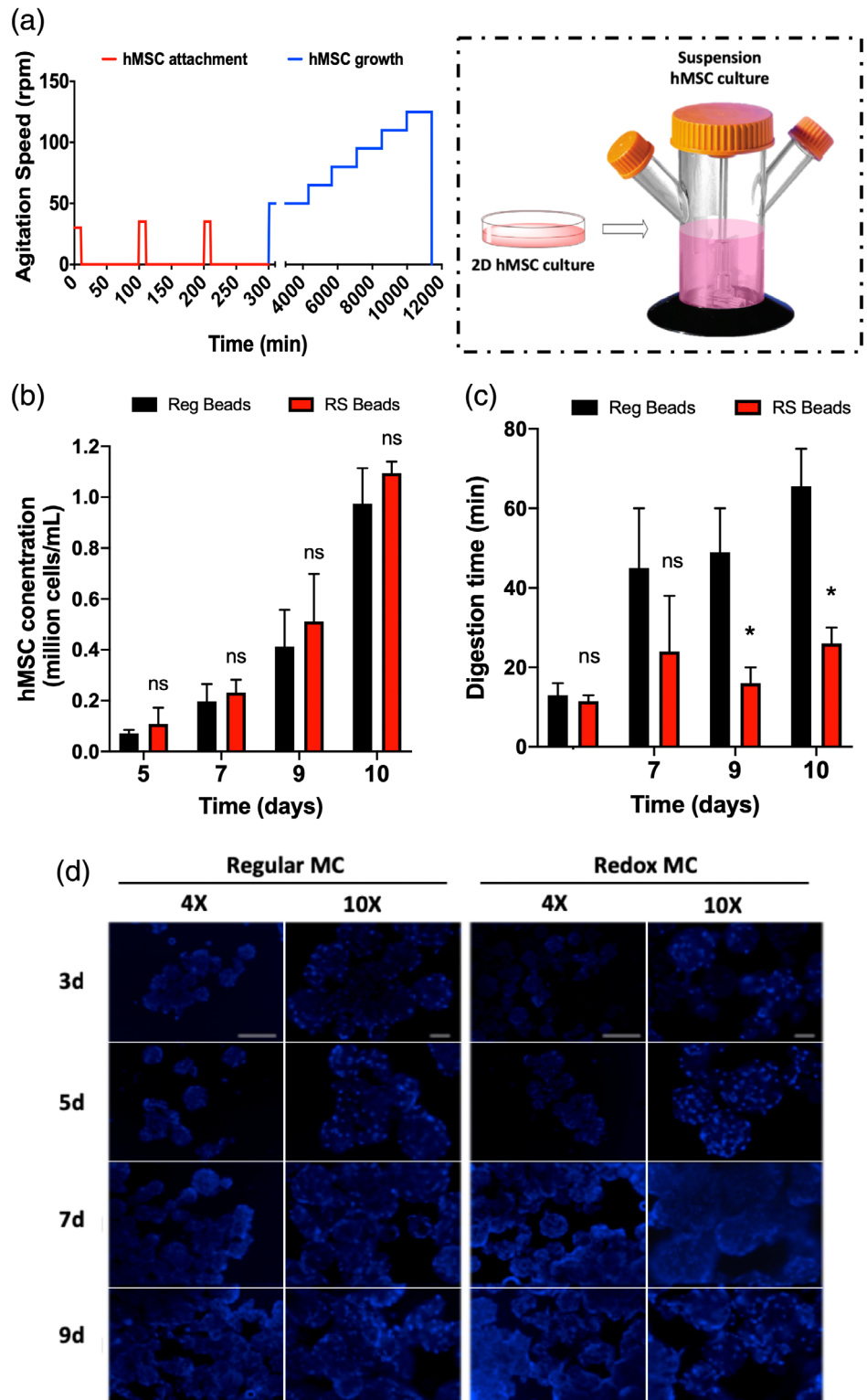


FIGURE 4 Redox-sensitive microcarriers degradation. (a) The degradation followed two distinct mechanisms facilitating rapid microcarriers dissolution. The disulfide bonds were cleaved by the reducing agent and the peptide bonds using a dissolution enzyme. Clzyme BP protease and Clzyme collagenase were used as enzyme at 0.5 U/ml and tris(2-carboxyethyl)phosphine hydrochloride (TCEP) was used as a reducing agent. (b) Dissolution time is shown for RS beads and Reg beads using different dissolution media. Results are shown as mean and SD of triplicates. Statistical significance was determined using Reg beads treated with 0.5 U/ml of enzyme as a control group (* $p < 0.05$). (c) Study of hMSC viability as a function of exposure time to the dissolution solution. Results are shown as mean and SD of triplicates. Statistical significance was determined using untreated cells a control group (* $p < 0.05$)

7. Results show that RS beads dissolved more quickly than the Reg beads (at least 15 times faster). The viable cell density (VCD) for the Reg beads plateaued around 15 volumes processed (Figure 7c), but aggregates continued to be observed through 23 volumes processed (Figure 7e). In contrast, less aggregates were observed for RS beads after one volume processed (Figure 7e). For the RS beads group, the microcarriers were dissolved rapidly enough that they were not visible by eye after the incubation period

(Figure 7f). The VCD curve for the RS beads also indicated that the cells had been released from their carriers almost immediately, as no increase in VCD was observed over the course of dissolution (Figure 7d). In addition to cell dissolution time, postdissolution viability was tested (NucleoCounter NC200) to evaluate cytotoxicity of the dissolution procedure. Figure 7g,h shows that no cell toxicity was observed in either of these harvests. In both cases, cell viability was higher than 90%.

FIGURE 5 Spinning cell culture of hMSC on Reg beads and RS beads. (a) The optimized protocol that was used for hMSC culture on the microcarriers. (b) Cell number during the spinning cell culture. Results are shown as mean and SD of triplicates. Statistical significance was determined using Reg beads as a control group(*p). (c) Microcarrier dissolution time at different time points. Results are shown as mean and SD of triplicates. Statistical significance was determined using Reg beads as a control group(*p). (d) Fluorescent imaging (DAPI staining) of hMSC on Reg beads and RS beads (Scale bar: 500 μm for 4X, and 100 μm for 10X)



4 | DISCUSSION

To efficiently scale-up hMSC production, a well-designed microcarrier which presents with high cell affinity and rapid cell recovery is needed. Recently, Cultispher-G beads, based on gelatin (Sun et al., 2010), have been reported to facilitate high cell affinity due to their chemical

structure which presents with RGD domains. In addition, Cultispher-G beads can be subjected to enzyme degradation, using proteases such as collagenase, in order to isolate the final cell population. However, as the cells grow and proliferate, they deposit ECM which makes it hard for the enzymes to penetrate—a process that increases significantly their dissolution time. Therefore, the design criteria are (a) forming microcarriers

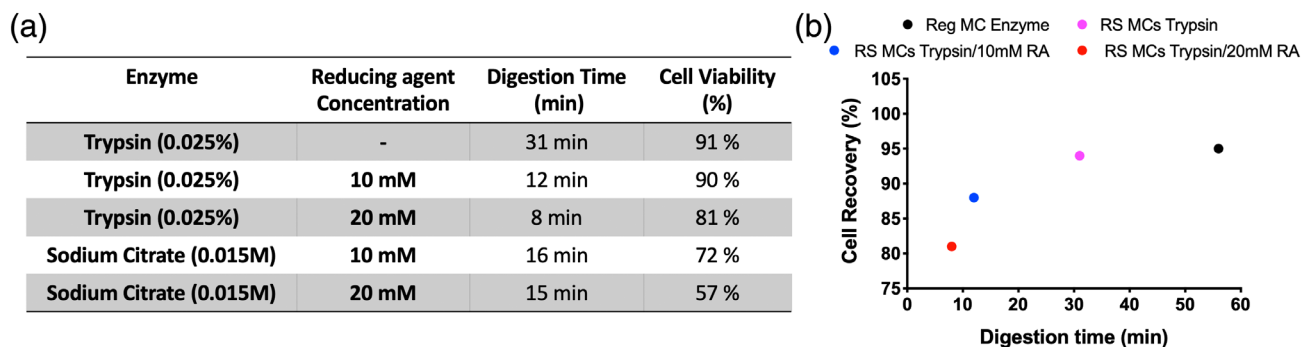


FIGURE 6 (a) Dissolution time and cell viability after complete dissolution of RS beads using various dissolution solutions. (b) Dissolution time and % cell recovery in selected dissolution solutions (RA represents reducing agent)

that dissolve considerably faster than standard Cultispher-G, while (b) maintaining similar growth kinetics and biocompatibility. To achieve that, RS beads were synthesized by their crosslinking with a redox-sensitive crosslinker, cystamine dihydrochloride. Its end-amine groups were converted to isocyanate (Figure 2a), allowing their reaction with the gelatin beads. Characterization of RS beads revealed that the chemical nature of the crosslinking moiety does not influence the final physicochemical properties of the resulting microcarriers. Our results prove that the RS beads and the Reg beads have similar crosslinking degree and hydrophilicity (Figure 3). In addition, RS beads presented lower dissolution time than Reg beads (6 min vs. 30 min) when a mixture of reducing agent and an enzyme was used. RS bead dissolution follows two distinct degradation mechanisms. First, the disulfide bonds in the redox-sensitive crosslinker are cleaved by reducing agents, such as TCEP. Then, the peptide bonds between amino acids are cleaved using enzymes, such as collagenase and proteases (Figure 4). Interestingly, Reg beads could no longer be fully dissolved in the same time frame they did in the presence of enzymes when we switched to the combination of reducing agent with enzymes as the dissolution solution. This is because the reducing agents are capable of denaturing both collagenase and proteases. Within a short period of time, only part of the enzyme remains active and hence can still affect the gelatin-based beads dissolution before being denatured by the reducing agents, thus facilitating the dissolution of the RS beads. However, in the case of Reg beads the enzyme was denatured before complete dissolution was achieved. In addition, RS beads showed a significantly faster dissolution using only an enzyme as a dissolution solution compared to the Reg beads (Figure 4b). The plausible reason is that the protease used in the enzyme dissolution solution is cysteine-based, and hence the enzyme can cleave the disulfide bonds.

Once the dissolution mechanism was characterized, we seeded hMSC on the microcarriers and allowed them to attach and proliferate in spinning flasks *in vitro*. RS beads enabled similar cell growth kinetics as that of the Reg beads, depicting an exponential cell growth within the first 4 days of incubation. Following hMSC attachment to the microcarriers (Day 4), the cells start depositing their own ECM to support their proliferation, as observed in Supplementary Figure S3. The high ECM deposition will result in a longer dissolution time compared

to the Reg beads without the cells (Figure 5c). Yet, when RS beads were used, lower dissolution times were achieved during the entire culture period. For instance, at Day 7 Reg beads were dissolved in 55 min and RS beads in 22 min. To further improve the microcarrier dissolution time in the presence of cells, different enzyme solutions were tested. When Trypsin (0.025%) was used instead of collagenase, RS beads dissolution time was further reduced from 22 to 8 min. Therefore, a mixture of Trypsin (0.025%) with 10 mM reducing agent was selected as a dissolution solution for the scale-up experiments.

The bioreactor experiments suggested cell growth may be slightly slower when culturing on RS beads, however, it is not considered significant since replicates of the control microcarrier process using identical conditions presents high variability (Figure 7a). In accordance with the spinner flasks data, RS beads were rapidly dissolved in a short period of time after 7–8 days of culture. This improved rate of dissolution was easily noticeable after a brief incubation without the use of mechanical aids (tubing assembly). The dissolution of RS beads is also more visibly complete, producing a single-cell suspension with fewer aggregates (Figure 7e). The best dissolution approach observed in bioreactors was achieved by adding reducing agent and enzymes simultaneously. A reducer-added-first approach was not as effective. This may suggest that the cells and/or the ECM they produce shield the microcarriers from the reducing agents. By adding the reagents simultaneously, the ECM and cells are removed from the surface of the beads, exposing them to the reducing agent. This would make their dissolution faster than standard Cultispher-G dissolved by enzymes alone, as the cells and ECM compete with the beads for the enzymes. These results suggest that our newly developed fast dissolving microcarriers enable overcoming one of the main limitations of cell harvesting; fast cell retrieval without affecting cell viability.

5 | CONCLUSIONS

We have successfully synthesized redox-sensitive gelatin-based microcarriers, with on-demand degradation. We demonstrated that

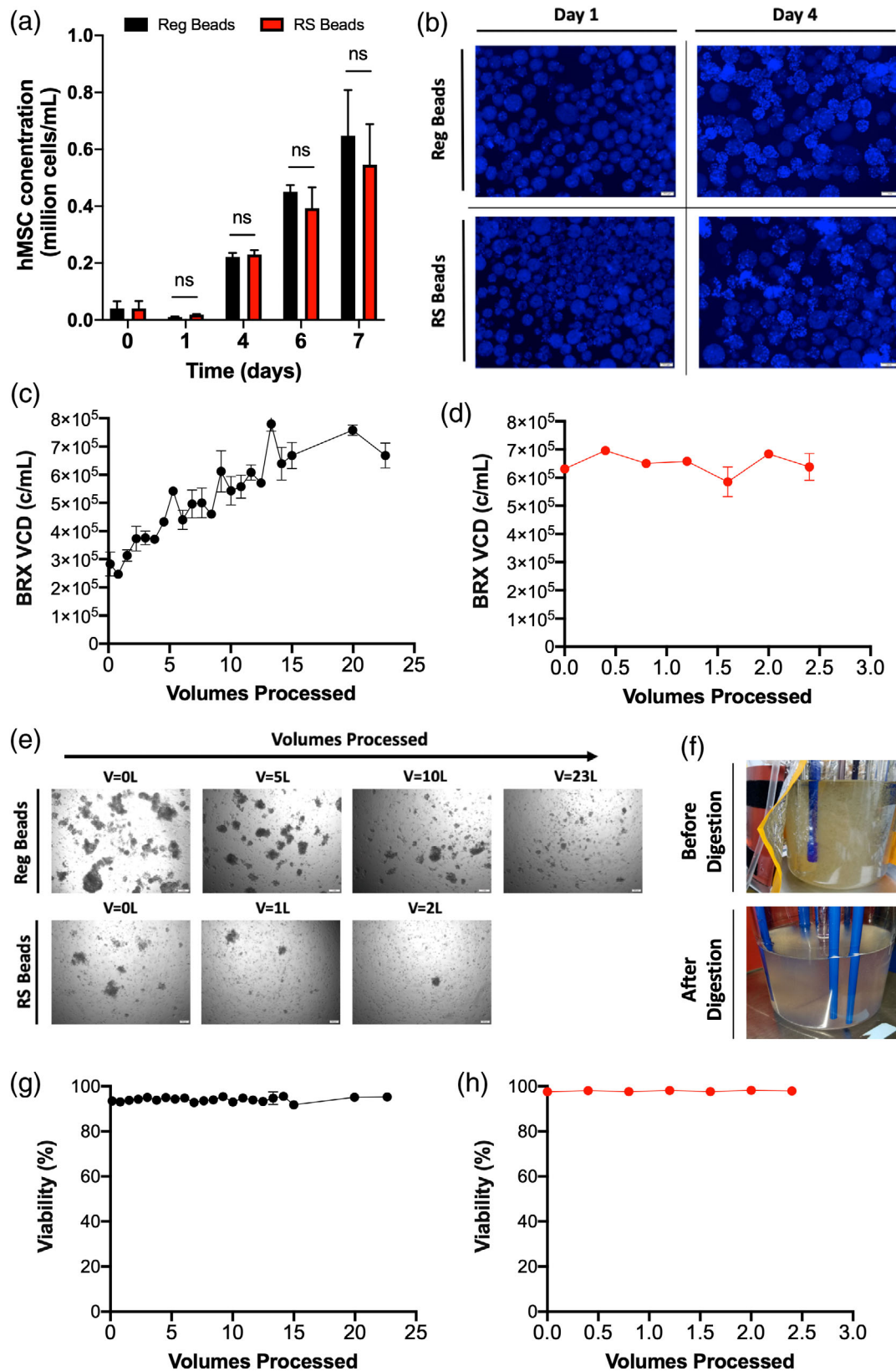


FIGURE 7 hMSC are produced in large-scale bioreactors using RS beads. (a) Viable cell density (VCD) of the bioreactors over culture duration. (b) hMSC nucleus staining with DAPI in Reg beads and RS beads on Day 1 (left) and Day 4 (right) (scale bar: 200 μ m [Day 1] and 1 mm [Day 4]). (c,d) VCD of hMSC in bioreactors over the course of microcarrier dissolution on Day 7 of culture using Reg and RS beads, respectively. (e) Microscope imaging of dissolved microcarriers on Day 7. Different volumes were processed for Reg beads and RS beads (scale bar: 200 μ m). (f) Bioreactor images of RS beads before and after dissolution. (g,h) Cell viability of hMSC in bioreactors over the course of microcarrier dissolution on Day 7 of culture using Reg beads and RS beads, respectively. Results are shown as mean and SD and statistical significance was determined by Mann-Whitney *U* test using Reg beads as a control group

the dissolution solution containing enzymes and a reducing agent, as well as the redox dissolution products are noncytotoxic. RS beads proved to be an effective cell carrier, here for hMSC. Most importantly, redox dissolution time for RS beads was significantly lower than enzymatic dissolution time for Reg beads after cell attachment and proliferation in spinner flasks. Finally, RS beads have been shown to reduce harvest time by at least 15-fold in bioreactors of 3 L. Therefore, RS beads present high potential as a cell carrier for scale-up cell manufacturing that can be used for cell therapy, permitting high cell proliferation and recovery yield.

ACKNOWLEDGMENTS

The authors thank Lonza for the collaboration and for funding the project. The authors also thank the Swanson Biotechnology Center at the Koch Institute for Integrative Cancer Research at Massachusetts Institute of Technology (MIT) for assistance with the microscopy core. Finally, the authors would also like to thank D. S. Yun for SEM-EDX assistance at the Peterson Nanotechnology Materials Core Facility.

CONFLICT OF INTEREST

The authors declare no potential conflict of interest.

REFERENCES

- Abbasi-Malati, Z., Roushandeh, A. M., Kuwahara, Y., & Roudkenar, M. H. (2018). Mesenchymal stem cells on horizon: A new arsenal of therapeutic agents. *Stem Cell Reviews and Reports*, 14(4), 484–499. <https://doi.org/10.1007/s12015-018-9817-x>
- Abdallah, B. M., & Kassem, M. (2009). The use of mesenchymal (skeletal) stem cells for treatment of degenerative diseases: Current status and future perspectives. *Journal of Cellular Physiology*, 218(1), 9–12. <https://doi.org/10.1002/jcp.21572>
- Bai, L., Shao, H., Wang, H., Zhang, Z., Chang, S., Dong, L., ... Zhang, X. (2017). Effects of mesenchymal stem cell-derived exosomes on experimental autoimmune uveitis. *Scientific Reports*, 7(1), 4323. <https://doi.org/10.1038/s41598-017-04559-y>
- Barczyk, M., Carracedo, S., & Gullberg, D. (2010). Integrins. *Cell and Tissue Research*, 339(1), 269–280. <https://doi.org/10.1007/s00441-009-0834-6>
- Bianco, P., Robey, P. G., & Simmons, P. J. (2008). Mesenchymal stem cells: Revisiting history, concepts, and assays. *Cell Stem Cell*, 2(4), 313–319. <https://doi.org/10.1016/j.stem.2008.03.002>
- Chen, A. K.-L., Chew, Y. K., Tan, H. Y., Reuveny, S., & Steve Kah Weng, O. (2015). Increasing efficiency of human mesenchymal stromal cell culture by optimization of microcarrier concentration and design of medium feed. *Cytotherapy*, 17(2), 163–173. <https://doi.org/10.1016/j.jcyt.2014.08.011>
- Davidenko, N., Schuster, C. F., Bax, D. V., Farnale, R. W., Hamaia, S., Best, S. M., & Cameron, R. E. (2016). Evaluation of cell binding to collagen and gelatin: A study of the effect of 2D and 3D architecture and surface chemistry. *Journal of Materials Science: Materials in Medicine*, 27(10), 148. <https://doi.org/10.1007/s10856-016-5763-9>
- dos Santos, F., Campbell, A., Fernandes-Platzgummer, A., Andrade, P. Z., Gimble, J. M., Wen, Y., ... Cabral, J. M. S. (2014). A xenogeneic-free bioreactor system for the clinical-scale expansion of human mesenchymal stem/stromal cells. *Biotechnology and Bioengineering*, 111(6), 1116–1127. <https://doi.org/10.1002/bit.25187>
- Hervy, M., Weber, J. L., Pecheul, M., Dolley-Sonneville, P., Henry, D., Zhou, Y., & Melkoumian, Z. (2014). Long term expansion of bone marrow-derived HMSCs on novel synthetic microcarriers in Xeno-free, defined conditions. *PLoS One*, 9(3), e92120. <https://doi.org/10.1371/journal.pone.0092120>
- Hourd, P., Ginty, P., Chandra, A., & Williams, D. J. (2014). Manufacturing models permitting roll out/scale out of clinically led autologous cell therapies: Regulatory and scientific challenges for comparability. *Cytotherapy*, 16(8), 1033–1047. <https://doi.org/10.1016/j.jcyt.2014.03.005>
- Kaiser, A. D., Assenmacher, M., Schröder, B., Meyer, M., Orentas, R., Bethke, U., & Dropulic, B. (2015). Towards a commercial process for the manufacture of genetically modified T cells for therapy. *Cancer Gene Therapy*, 22(2), 72–78. <https://doi.org/10.1038/cgt.2014.78>
- Lai, R. C., Arslan, F., Lee, M. M., Sze, N. S. K., Choo, A., Chen, T. S., ... Lim, S. K. (2010). Exosome secreted by MSC reduces myocardial ischemia/reperfusion injury. *Stem Cell Research*, 4(3), 214–222. <https://doi.org/10.1016/j.scr.2009.12.003>
- Lambrechts, T., Sonnaert, M., Schrooten, J., Luyten, F. P., Aerts, J. M., & Papanitoniou, I. (2016). Large-scale mesenchymal stem/stromal cell expansion: A visualization tool for bioprocess comparison. *Tissue Engineering - Part B: Reviews*, 22(6), 485–498. <https://doi.org/10.1089/ten.teb.2016.0111>
- Lee, R. H., Pulin, A. A., Seo, M. J., Kota, D. J., Ylostalo, J., Larson, B. L., ... Prockop, D. J. (2009). Intravenous HMSCs improve myocardial infarction in mice because cells embolized in lung are activated to secrete the anti-inflammatory protein TSG-6. *Cell Stem Cell*, 5(1), 54–63. <https://doi.org/10.1016/j.stem.2009.05.003>
- Múnoz, Z., Shih, H., & Lin, C.-C. (2014). Gelatin hydrogels formed by orthogonal thiol-norbornene photochemistry for cell encapsulation. *Biomaterials Science*, 2(8), 1063–1072. <https://doi.org/10.1039/C4BM00070F>
- Ng, Y.-C., Berry, J. M., & Butler, M. (1996). Optimization of physical parameters for cell attachment and growth on macroporous microcarriers. *Biotechnology and Bioengineering*, 50(6), 627–635. [https://doi.org/10.1002/\(SICI\)1097-0290\(19960620\)50:6<627::AID-BIT3>3.0.CO;2-M](https://doi.org/10.1002/(SICI)1097-0290(19960620)50:6<627::AID-BIT3>3.0.CO;2-M)
- Nguyen, B.-N. B., Ko, H., & Fisher, J. P. (2016). Tunable osteogenic differentiation of HMPs in tubular perfusion system bioreactor. *Biotechnology and Bioengineering*, 113(8), 1805–1813. <https://doi.org/10.1002/bit.25929>
- Nienow, A. W., Rafiq, Q. A., Coopman, K., & Hewitt, C. J. (2014). A potentially scalable method for the harvesting of HMSCs from microcarriers. *Biochemical Engineering Journal*, 85(April), 79–88. <https://doi.org/10.1016/j.bej.2014.02.005>
- Nold, P., Brendel, C., Neubauer, A., Bein, G., & Hackstein, H. (2013). Good manufacturing practice-compliant animal-free expansion of human bone marrow derived mesenchymal stroma cells in a closed hollow-fiber-based bioreactor. *Biochemical and Biophysical Research Communications*, 430(1), 325–330. <https://doi.org/10.1016/j.bbrc.2012.11.001>
- Pittenger, M. F. (1999). Multilineage potential of adult human mesenchymal stem cells. *Science*, 284(5411), 143–147. <https://doi.org/10.1126/science.284.5411.143>
- Prockop, D. J. (2007). 'Stemness' does not explain the repair of many tissues by mesenchymal stem/multipotent stromal cells (MSCs). *Clinical Pharmacology & Therapeutics*, 82(3), 241–243. <https://doi.org/10.1038/sj.cpt.6100313>
- Romanov, Y. A. (2003). Searching for alternative sources of postnatal human mesenchymal stem cells: Candidate MSC-like cells from umbilical cord. *Stem Cells*, 21(1), 105–110. <https://doi.org/10.1634/stemcells.21-1-105>
- Salmikangas, P., Menezes-Ferreira, M., Reischl, I., Tsiftoglou, A., Kyselovic, J., Borg, J. J., ... Schneider, C. K. (2015). Manufacturing, characterization and control of cell-based medicinal products: Challenging paradigms toward commercial use. *Regenerative Medicine*, 10(1), 65–78. <https://doi.org/10.2217/rme.14.65>
- Sheridan, C. (2018). First off-the-shelf mesenchymal stem cell therapy nears European approval. *Nature Biotechnology*, 36(3), 212–214. <https://doi.org/10.1038/nbt0318-212a>

- Sigurdsson, S. T., Seeger, B., Kutzke, U., & Eckstein, F. (1996). A mild and simple method for the preparation of isocyanates from aliphatic amines using trichloromethyl chloroformate. Synthesis of an isocyanate containing an activated disulfide. *The Journal of Organic Chemistry*, 61(11), 3883–3884. <http://www.ncbi.nlm.nih.gov/pubmed/11667245>
- Squillaro, T., Peluso, G., & Galderisi, U. (2016). Clinical trials with mesenchymal stem cells: An update. *Cell Transplantation*, 25(5), 829–848. <https://doi.org/10.3727/096368915X689622>
- Stephenson, M., & Grayson, W. (2018). Recent advances in bioreactors for cell-based therapies. *F1000Research*, 7(April), 517. <https://doi.org/10.12688/f1000research.12533.1>
- Sun, L.-Y., Hsieh, D.-K., Syu, W.-S., Li, Y.-S., Chiu, H.-T., & Chiou, T.-W. (2010). Cell proliferation of human bone marrow mesenchymal stem cells on biodegradable microcarriers enhances in vitro differentiation potential. *Cell Proliferation*, 43(5), 445–456. <https://doi.org/10.1111/j.1365-2184.2010.00694.x>
- Varley, M. C., Markaki, A. E., & Brooks, R. A. (2017). Effect of rotation on scaffold motion and cell growth in rotating bioreactors. *Tissue Engineering Part A*, 23(11–12), 522–534. <https://doi.org/10.1089/ten.tea.2016.0357>
- Wei, X., Xue, Y., Han, Z. P., Fang Fang, Q., Shao, L., & Shi, Y. F. (2013). Mesenchymal stem cells: A new trend for cell therapy. *Acta Pharmacologica Sinica*, 34(6), 747–754. <https://doi.org/10.1038/aps.2013.50>
- Wu, S., Liu, C., & Lian, W. (2004). Optimization of microcarrier cell culture process for the inactivated enterovirus type 71 vaccine development. *Vaccine*, 22(29–30), 3858–3864. <https://doi.org/10.1016/j.vaccine.2004.05.037>
- Yang, H. S., Jeon, O., Bhang, S. H., Lee, S.-H., & Kim, B.-S. (2010). Suspension culture of mammalian cells using thermosensitive microcarrier that allows cell detachment without proteolytic enzyme treatment. *Cell Transplantation*, 19(9), 1123–1132. <https://doi.org/10.3727/096368910X516664>
- Zuk, P. A., Zhu, M., Ashjian, P., de Ugarte, D. A., Huang, J. I., Mizuno, H., ... Hedrick, M. H. (2002). Human adipose tissue is a source of multipotent stem cells. *Molecular Biology of the Cell*, 13(12), 4279–4295. <https://doi.org/10.1091/mbc.e02-02-0105>

SUPPORTING INFORMATION

Additional supporting information may be found online in the Supporting Information section at the end of this article.

How to cite this article: Dosta P, Ferber S, Zhang Y, et al. Scale-up manufacturing of gelatin-based microcarriers for cell therapy. *J Biomed Mater Res*. 2020;1–13. <https://doi.org/10.1002/jbm.b.34624>